Journal of Applied Polymer Science

Continuous aligned poly(*meta*-phenylene isophthalamide) fibers via stable jet electrospinning

Weiwang Chen, Wenguo Weng
Institute of Public Safety Research, Department of Engineering Physics, Tsinghua University, Beijing, 100084, People's Republic of China
Correspondence to: W. Weng (E-mail: wgweng@tsinghua.edu.cn)

ABSTRACT: Continuous aligned poly(*meta*-phenylene isophthalamide) (PMIA) fibers are first fabricated by Stable Jet Electrospinning (SJES) with a collection distance of 15 cm. The unfolded length of every single fiber is calculated to be several hundred to several thousand meters. Morphology analysis by field emission scanning electron microscopy (FE-SEM) shows that these fibers are well arranged and uniformly distributed and their average fiber diameters decrease gradually with increasing collection speed. The effects of ambient temperature and humidity on the duration of stable jet are also discussed. Moderate temperatures and humidity are preferred for fabricating PMIA fibers with ultra-long size. Besides, the changes of the thermal and crystalline properties of PMIA fibers are also investigated. The significant decline in crystallinity should be responsible for its decreased thermal property. Further improvements to its thermal and crystalline performance must be given consideration in future applications. © 2016 Wiley Periodicals, Inc. J. Appl. Polym. Sci. **2016**, *133*, 43690.

KEYWORDS: crystallization; fibers; morphology; thermal properties

Received 3 December 2015; accepted 21 March 2016
DOI: 10.1002/app.43690

INTRODUCTION

Nano- and micron-sized fibers have attracted wide attention as functional materials over the recent years owing to their superior performances, such as high aspect ratio, large specific surface, diversified structures, and so on.[1–3] Electrospinning is a simple, convenient, and versatile technology to produce ultrafine fibers with diameters ranging from tens of nanometers to several microns.[4–7] After adding a proper high voltage to the cuspidate spinneret, the surface tension of spinning solution is overcame and an electrically charged liquid jet is ejected. As a result of electrostatic repulsion, ultrafine fiber will be finally formed by whipping and splitting processes.[8] Nonwoven fabrics, highly oriented fibers and continuous twisted yarns fabricated by electrospinning have been widely reported over the past few decades.[9–11]

With the development of electrospinning technology, Stable Jet Electrospinning (SJES) has emerged as a fascinating approach for fabricating individual fibers or well-aligned unidirectional fiber arrays by using a rotating cylindrical collector.[12] The characteristic whipping motion of the liquid jet can be suppressed or eliminated by introducing an auxiliary electrode, using special solvents or formulating the viscoelasticity of spinning dopes.[13–16] Carnell *et al.* applied an auxiliary electrode in their electrospinning setup to eliminate its instability by controlling the electric field and succeeded in obtaining stable liquid jet.[13] Zhou *et al.* studied the influence of some pivotal parameters including solvent, polymer molecular weight, and concentration on the property of stable jet when fabricating poly(L-lactic acid) (PLLA) fibers.[15] Experimental results revealed that the high viscoelasticity of polymer solution as well as low solvent dielectric constant should be the major contributor to the formation of single linear jet without bending instability. Similar results were also observed according to the research of Liu *et al.*[16] That is, the critical stable jet can be finally achieved by regulating the manufacturing parameters and the properties of spinning polymer solutions.

Because of its excellent thermal resistance, flame retardant effects, and great mechanical properties, poly(*meta*-phenylene isophthalamide) (PMIA) is being widely used as the main material of fire protective clothing, insulation paper, heat-resistant filters, etc. Nevertheless, few studies on the electrospinning of PMIA superfine fibers have been reported. Yao *et al.* discussed the spinnability of PMIA nanofibers in different solvents and pointed out that the lithium chloride/*N*,*N*-Dimethylacetamide (LiCl/DMAC) solvent system is a better choice for fabricating PMIA ultrafine fibers with preferable morphology and good mechanical properties.[17] Additionally, enhanced PMIA fibers with multi-walled carbon nanotubes (MWNTs) as the additives

were successfully fabricated by He *et al.*[18] Experimental results showed that the MWNTs were well aligned along the fibers and their mechanical properties were significant improved accordingly. Besides, the adsorption and breathable properties of electrospun PMIA nonwovens were also studied in the past few years.[19–22] However, little work on the fabrication of continuous aligned PMIA fibers with ultra-long length by electrospinning has been reported.

In this study, original PMIA solution with high viscosity and conductivity is used to get a stable liquid jet. Continuous aligned PMIA fibers are prepared first in one step by SJES using a rotating cylinder as the collector. The morphology and element composition of the resulting fibers are characterized by field emission scanning electron microscopy (FE-SEM). Morphology analysis shows that these fibers are well arranged and uniformly distributed with diameters from hundreds of nanometers to a few microns, much smaller than the commercial ones. Besides, the effects of ambient temperature and humidity on the duration of stable jet are discussed. The thermal and crystalline properties of PMIA fibers before and after electrospinning are also investigated by thermogravimetic analyzer (TGA) and X-ray diffraction (XRD), respectively. The stable jets obtained in the present study are expected to facilitate the fabrication of functional PMIA fibers with core-sheath, porous or other specific structures.

EXPERIMENTAL

Materials

Commercial PMIA fibers were supplied by Wanhua Chemical Group Co., (Yantai, China) with an annotated approximate molecular weight of 200,000 g mol^{-1}. *N,N*-Dimethylacetamide (DMAc) and lithium chloride (LiCl) purchased from Sinopharm Chemical Reagent Co., (Beijing, China) were used as received without further purification.

Electrospinning Process

A 15.8 wt % PMIA solution in DMAC with 5.6 wt % LiCl inside was selected as the original spinning solution. Vacuum dried LiCl (1.12 g) was first added into DMAC (15.72 g) to be completely dissolved under magnetic stirring. Then, 3.16 g commercial PMIA fibers, which were dried at 80 °C for 12 h in vacuum oven, were added into the above LiCl/DMAC ionic liquid with periodic stirring at 60 °C to reach a final homogenous solution. Spinning equipment (ET-2535) purchased from Ucalery Beijing Co., was used here to fabricate continuous ultra-long PMIA fibers. A 1mL plastic syringe was placed onto the feeding pump as the solution reservoir and a spinning needle ($21^{\#}$) with an inner diameter of 0.5 mm was attached to the positive electrode of the high voltage power supply. During the experiment, the solution feeding rate and electrospinning voltage were maintained at about 12.5 μL h^{-1} and 7.5 kV, respectively. A cylindrical collector (diameter of 10 cm, length of 35 cm) with different given rotating speeds was placed at a distance of 15 cm from the tip of the spinneret.

Characterization

The morphology and element composition of the fabricated continuous fibers were observed by field emission scanning electron microscopy (FE-SEM, SU-8010, Hitachi, Japan) equipped with energy dispersive X-ray spectroscopy (EDX). Prior to the observation, all specimens were coated with platinum for 60 s by an ion coater (IB-3, Eiko, Japan) to render them electrically conductive. The fiber diameter distribution and average fiber diameter were analyzed statistically based on the SEM results. At least 100 randomly selected fibers were used for each sample.

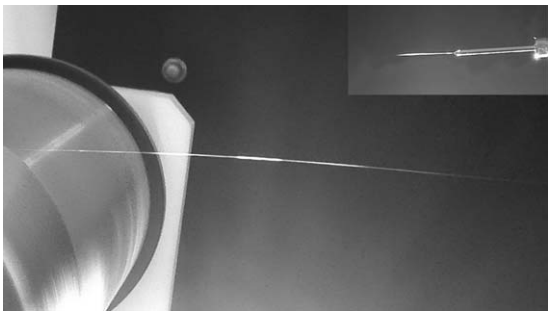

Figure 1. The spinning process of continuous aligned PMIA fibers.

The thermal properties of PMIA fibers were also measured using a thermogravimetric analyzer (TGA, TGA/DSC1/1600HT, Mettler-Toledo, Switzerland) from room temperature to 700 °C at a heating rate of 20 °C min^{-1} under nitrogen atmosphere. Besides, the crystallinities of the commercial and electrospun PMIA fibers were also characterized by X-ray diffraction (XRD, D8 Advance, Bruker, Germany) with a Ni-filtered Cu Kα radiation source at 40 kV and 40 mA ($\lambda = 1.5406$ Å).

RESULTS AND DISCUSSION

As a highly crystallized polymer, PMIA is almost insoluble in common solvents due to its high conjugation of molecular chains. However, the solubility of PMIA in DMAC can be greatly improved after adding a certain amount of chlorinated salt (LiCl or $CaCl_2$ in most cases). Of the two, LiCl is proved to be better for fabricating PMIA ultrafine fibers with preferable properties.[17] In the present study, a 15.8 wt % PMIA solution in DMAC with 5.6 wt % LiCl inside is tested to be optimal and is selected as the original solution for fabricating continuous aligned PMIA fibers.

The spinning process of continuous ultra-long PMIA fibers can be seen in Figure 1. After adding a proper high voltage of 7.5 kV to the cuspidate spinneret, the surface tension of the spinning droplet is overcame and an electrostatically driven jet with little whipping and no splitting is ejected. As can be seen from the figure, the spinning droplet, also known as Taylor cone, shows good conical structure. Moreover, only one single fiber is formed between the spinneret and the collector. The spinning solution's high viscosity and conductivity should be responsible. Under the auxiliary light, the stable jet can be easily captured and monitored on real time. During electrospinning, a collection speed ranging from 80 to 120 rpm is used to avoid reverse growth of PMIA fibers. With the help of rotating collector, continuous aligned PMIA fibers are finally obtained.

Fiber Morphology

All the PMIA fibers in Figure 2 are fabricated under room temperature (29.6 ± 0.7 °C) and 58 ± 4% humidity. Among them,

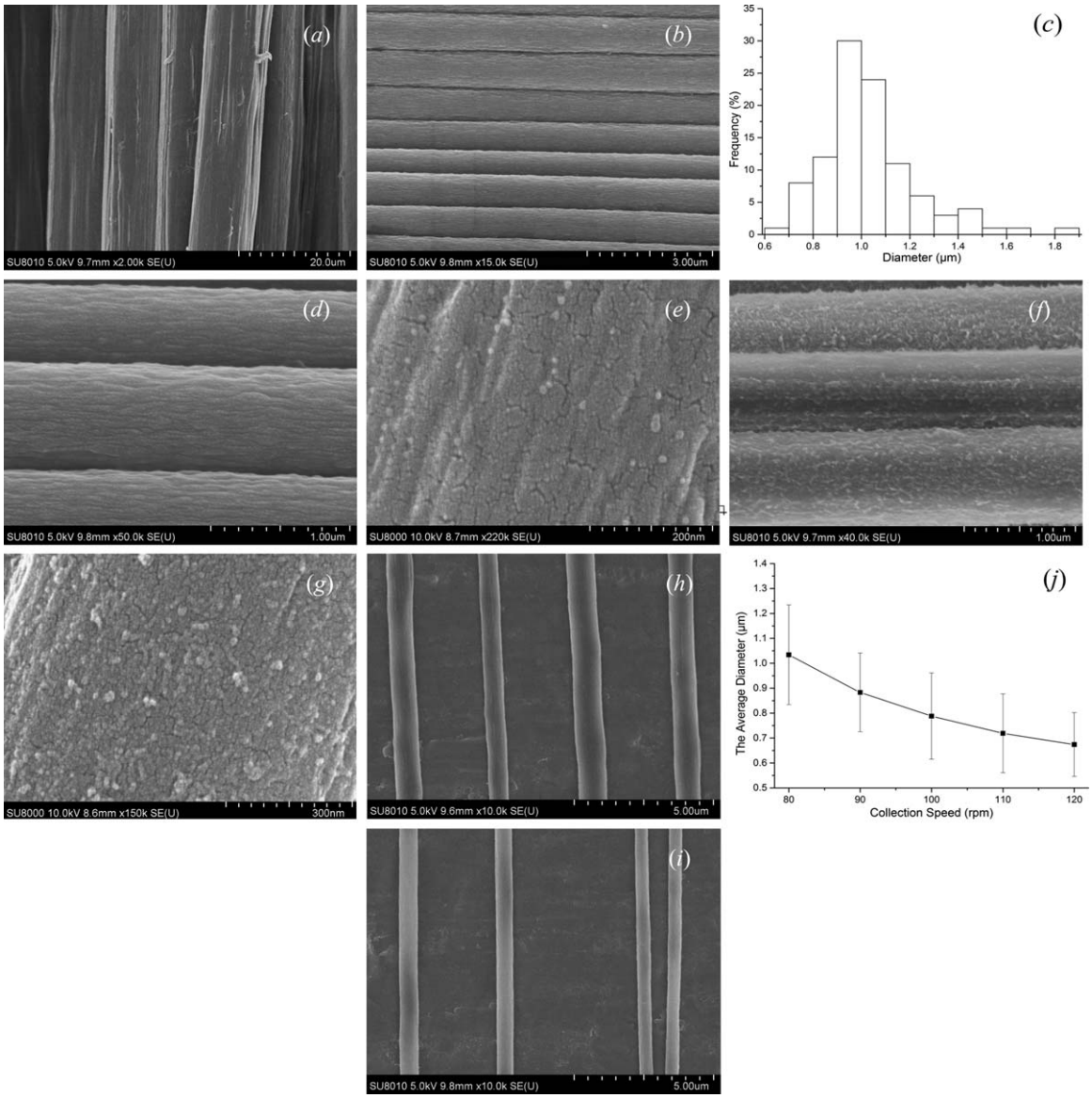

Figure 2. The morphology of PMIA fibers: (a,b) are the SEM micrographs of the commercial and the just-fabricated electrospun PMIA fibers; (c) is the fiber distribution of the aligned PMIA fibers; (d,e) and (f,g) are the enlarged images of the aligned PMIA fibers before and after water treatment for 24 h, respectively; (h,i) are the representative SEM images of PMIA fibers obtained under different rotating speeds (90 and 120 rpm, respectively); and (j) is the average fiber diameters varying with collection speed.

the continuous fibers in Figure 2(b–g) are prepared under the collection speed of 80 rpm. As shown, the commercial and ultrafine electrospun PMIA fibers without water treatment are well arranged and uniformly distributed. Compared with that during Near-Field Electrospinning (NFES),[23,24] longer collection distance usually results in more adequate volatilization of solvents. Little conglutination problem is observed among the target PMIA fibers owing to the long collection distance of 15 cm. The diameters of the obtained fibers range from hundreds of nanometers to a few microns, and the diameter distribution obeys normal distribution approximately. The average diameter of these ultrafine fibers is calculated to be 1.07 μm, much smaller than that of the commercial ones with an average diameter of 12.17 μm. Figure 2(b,d) shows that the just-fabricated fibers have relatively smooth surfaces with a lot of wrinkles upon them. In addition, there also exist some cracks and small particles on the fiber surfaces [see the enlarged image in Figure 2(e)]. Due to the strong moisture absorbability of LiCl, the formation of these particles and wrinkles may results from water swelling effect under such a high ambient humidity. After immersed in water for 24 h, the fibers are more or less shrunk by extracting LiCl in the fibers and the average diameter is reduced to 1.03 μm. Scanning electron microscopy (SEM) analysis also shows that the washed fibers become much rougher with a large amount of small floccules and particles, as shown in Figure 2(f,g). However, no obvious pores are observed.

Figure 2(h,i) are the representative SEM images of aligned PMIA fibers under different collection speeds. Since a

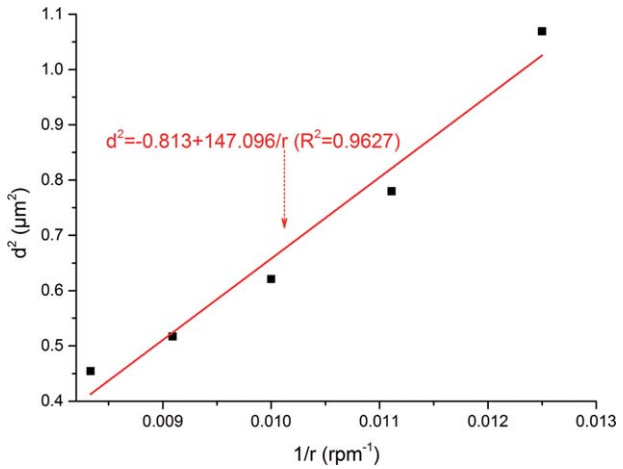

Figure 3. The relationship between d^2 and r^{-1}. [Color figure can be viewed in the online issue, which is available at wileyonlinelibrary.com.]

reciprocating horizontal speed of 2 cm min^{-1} is used in the course of experiment, shorter collection time inevitably results in lower fiber density. The average fiber diameter under 90 rpm is calculated to be 0.88 μm, which is 0.19 μm thinner than that under 80 rpm. With increasing rotating speed, further decrease in fiber diameter is found. The average fiber diameter is reduced to 0.67 μm when the collection speed reaches 120 rpm. As seen from the curve in Figure 2(j), the average diameter of PMIA fibers is a monotonically decreasing function of collection speed. The significant decrease in fiber diameter is largely thanks to the stretching effect of cylindrical collector. Therefore, there is reason to believe that ultrafine fibers with much smaller diameters can also be successfully prepared under a faster rotating speed.

Fiber Length

During electrospinning, the fabrication of single electrospun PMIA fiber lasted tens of minutes to several hours without any interruption. The totally unfolded length of every ultra-long fiber, expressed as L, is calculated to be several hundred to several thousand meters according to eq. (1):

$$\text{length } (L) = \pi Drt \quad (1)$$

where π is the transcendental number of pi, D and r (rpm) are the diameter and rotating speed of the cylindrical collector, respectively, and t is the duration of one single fiber without interruption.

Considering the constant extrusion rate of spinning solution, the volume of electrospun PMIA fibers per unit time (V) can be recognized as a fixed value. To simplify computing, the fabricated fibers are considered to be a long thin cylinder with the same diameter of d. Thus, the square of fiber diameter should be inversely proportional to the collection speed r, as explained below.

$$V = \pi(d/2)^2 \times L/t = 0.25\pi^2 d^2 Dr = \text{Constant} \quad (2)$$

Taking the average fiber diameter as the cylinder diameter d, the relationship between d^2 and r^{-1} together with the linear fitting equation is plotted in Figure 3. From the figure it can be seen that d^2 has good linear relationship with r^{-1}. The fitting result further illustrates that much finer fibers with smaller diameters will be successfully prepared under faster rotating speeds.

In addition to solution properties, the values of ambient temperature and humidity are also important to the duration of stable jet, unfolded length of PMIA fibers in other words. The changes of fiber duration with ambient temperature and humidity are plotted in Figure 4. During the experiment, the temperature in the environmental chamber is adjustable and remains approximately constant over time with minor fluctuations. In addition, the ambient humidity in the chamber is regulated by the humidity control system including an industrial humidifier (YDH-803EB, Parkoo) and a dehumidifier (BL-860S, Belin). As shown in Figure 4(a,b), the average time of duration shows a first increase and then decrease tendency with the increase of humidity, while the duration of continuous PMIA fibers decreases gradually as the temperature rises. Generally, the viscosity of polymer droplet will increase gradually as the solvent evaporates with increasing temperature and decreasing humidity. The fabrication of single PMIA fiber will be eventually interrupted when the spinning solution get too viscous to stretch. Conversely, ribbon-like structures and conglutination problem among fibers may occur at low temperatures due to the

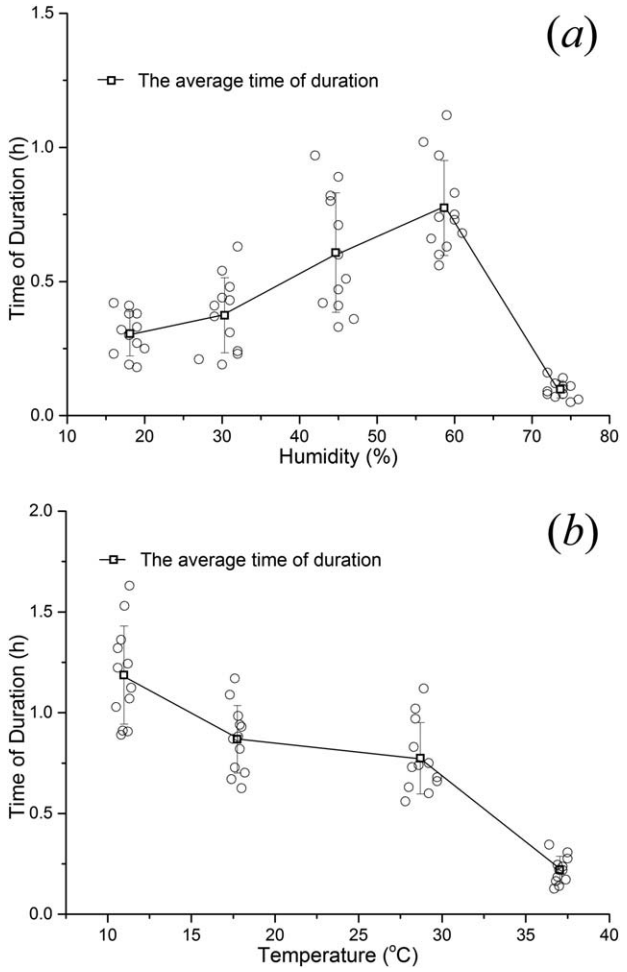

Figure 4. The variations of fiber duration with ambient (a) humidity and (b) temperature.

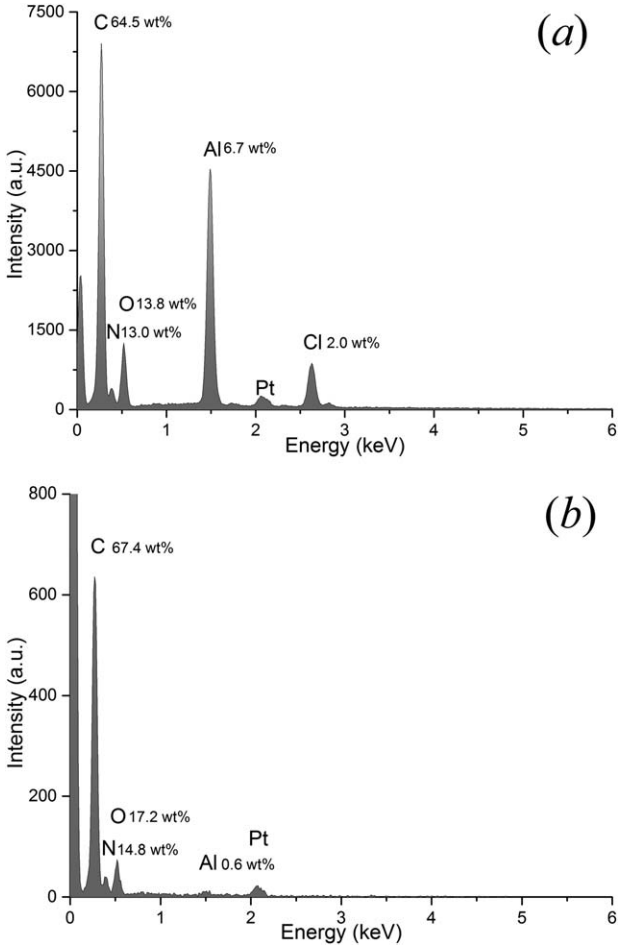

Figure 5. Point-scanning results about the element composition of the fabricated PMIA fibers (a) before and (b) after water extraction.

insufficient vitalization of solvent. Besides, excessive humidity exposure will also result in the precipitation and solidification of PMIA for the strong moisture absorbability of LiCl. The color change of the Taylor cones from transparent to white under high humidity conditions is living proof of the precipitation of surface PMIA. Because of this, a significant drop in fiber duration is observed, from about 45 to 6 min as the ambient humidity increases from 58 to 74% [see Figure 4(b)]. It should be noted that the fluidity of the pinning solution increase with increasing temperature, and the end of the stable fiber jet tends to suffer more obvious whipping process at higher temperatures.

In practical operations, ambient temperature and humidity do play an important role in fabricating ultrafine PMIA fibers. These factors as well as solution properties affect and restrict each other. There is usually a relatively narrow set of manufacturing conditions that can provide optimum results. With the given PMIA spinning solution, moderate temperature and humidity are preferred for fabricating PMIA fibers with ultra-long size.

EDX Analysis

The element composition of the fabricated PMIA fibers before and after water treatment is observed by FE-SEM equipped with EDX. The point-scanning results can be seen in Figure 5. As the PMIA fibers are made up of carbon, hydrogen, nitrogen, and oxygen elements, these elements certainly account for the majority of all components. Regardless of the coated platinum, a certain amount of aluminum and chlorine is also detected. However, as such a light metal, lithium element cannot be detected by this technology due to the limited threshold of EDX. After immersed in water, the relative contents of carbon, nitrogen, and oxygen do not seem to change much. While the content of aluminum remaining from the aluminum foils and specimen stage shows a dramatic decrease. A significant reduction in chlorine content is also observed due to the high solubility of chlorinated salt in water and no surface chlorine element is detected after water extraction. It is reasonable to believe that the residual LiCl in the continuous electrospun PMIA fibers is washed clean.

Thermal Properties

The thermal behaviors of the commercial and continuous electrospun PMIA fibers were also studied by TGA in nitrogen atmosphere. The results are shown in Figure 6. It can be seen from the curves (a) and (b) that a weight loss of 5–8 wt % is observed for both fibers before 150 °C, which is attributed to the removal of possible residual solvent (DMAC) and moisture. After that, almost no decomposition process occurs before 400 °C for the commercial fibers. Somewhat differently, a slight gradual weight loss process within the same temperature range is observed for the electrospun ones. Due to the cleavage of hydrogen bonds and crystal structures at high temperatures, the main degradation process for both fibers starts at about 400 °C. As with previous studies, the thermal degradation of PMIA fibers is a complex process involving polymer rupture and rearrangement reactions.[25–28] From the derivative thermogravimetric (DTG) curves in the figure, more than two mass loss peaks are found for the commercial PMIA fibers above 400 °C. Among them, the first weight loss peak shows an onset temperature of 400 °C and ends at about 480oC where another new peak begins. The two decomposition steps within the temperature range of 400 to 600 °C correspond to the polymer heterolysis and hemolysis, respectively.[26] When the temperature is over

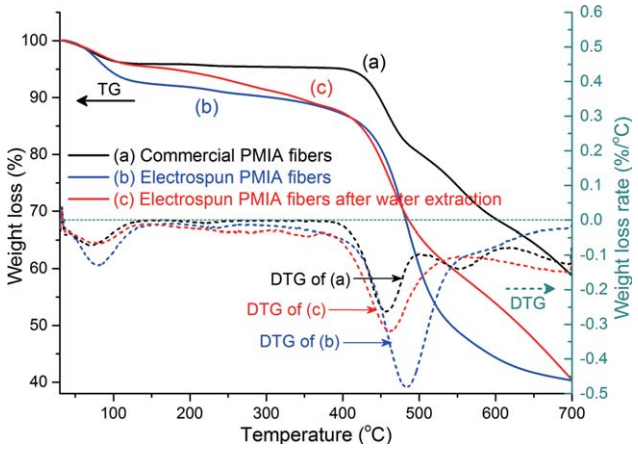

Figure 6. TG and DTG curves of the commercial and continuous aligned electrospun PMIA fibers. [Color figure can be viewed in the online issue, which is available at wileyonlinelibrary.com.]

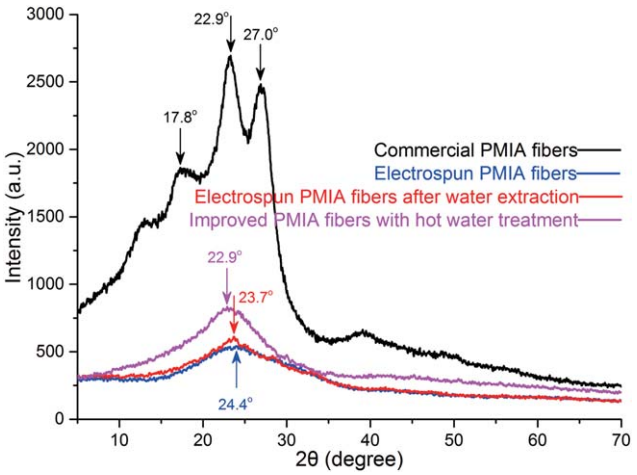

Figure 7. XRD patterns of the commercial and continuous aligned electrospun PMIA fibers. [Color figure can be viewed in the online issue, which is available at wileyonlinelibrary.com.]

600 °C, dehydrogenation and condensation reactions take place and aromatic compounds are yielded accordingly.[26,27] For the electrospun PMIA fibers, however, only one thermal degradation peak is observed from the derivative curve of (b). In addition, the residue of electrospun PMIA fibers at 700 °C is approximately 44 wt % on dry basis and 18 wt % lower than that of the commercial fibers. Thus differences may result from the disordered arrangement of PMIA molecules and the heterogeneity of electrospun fibers with LiCl inside.

After water exaction, the moisture absorption of the processed fibers is reduced significantly because of the removal of hygroscopic LiCl. The reduced water content in these fibers leads to a weakened weight loss process before 150 °C, as shown in Figure 6. The removal of salt is also expected to result in a stronger conjugation among PMIA chains due to the recovery of intermolecular hydrogen bonds. However, the TG curve shows a more significant degradation process between 150 and 460 °C after water exaction, expressed as higher weight loss rate. This is most probably because of the thermal degradation of small floccules and particles upon the fiber surfaces. Even so, the main degradation process for the water-treated fibers still starts at about 400 °C, which is consistent with two other fibers. With the further increase of temperature, the pyrolysis of the washed PMIA fibers is largely restricted until 560 °C by comparison to the unwashed fibers. Then a more dramatic weight loss process is observed above 600 °C, similar to the thermal behavior of the commercial PMIA fibers. The removal of LiCl in these fibers should be responsible for the differences and further studies are needed to explore the specific effect of LiCl on the pyrolysis mechanism of PMIA fibers.

Crystalline Characteristics

The XRD patterns of the commercial and electrospun PMIA fibers are shown in Figure 7. Since the commercial fibers are usually produced by intensive drawing at high temperatures,[29] highly crystallized PMIA fibers with an ordered molecular arrangement will be finally obtained. XRD spectra of the commercial fibers show three main diffraction peaks at the scattering angle of 17.8°, 22.9°, and 27.0°. However, only one greatly weakened peak at 24.4° is found for the electrospun ones. That is, the crystallinity of ultrafine electrospun PMIA fibers decreases sharply and a phase between amorphous and highly crystallized structures is formed. This is why the electrospun PMIA fibers suffer an obvious decline in thermal stability. The appearance of a largely degenerated crystallization peak may be caused by the faint stress-induced crystallization during electrospinning.[18] The stretching effect of the rotating collector is also believed to have positive effects on its crystallization. After washing, the crystallinity of the electrospun PMIA fibers is slightly enhanced with a fronted peak at 23.7°. However, the differences are very small. It illustrates that the post water treatment has little influence on the crystallinity of electrospun PMIA fibers.

Further modifications by post heat and microwave treatments or adding reinforced materials, etc. should be considered to improve the crystallization and comprehensive properties of PMIA fibers in future applications.[18,22,30] In this study, the prepared PMIA fibers are treated with tension (2000 N) in hot water (80 °C) for 2 h to improve their crystallinity. The result shows that the crystallinity of the treated PMIA fibers is obviously enhanced and the peak moves forward to 22.9°. Compared with the commercial ones, however, the crystallinity of these fibers still needs to be further improved. Longer treatments with greater tension should be helpful.

CONCLUSIONS

In this study, continuous aligned PMIA fibers with a totally unfold length of several hundred to several thousand meters are successfully fabricated by SJES. Morphology analysis shows that the electrospun fibers are well arranged and uniformly distributed with diameters from hundreds of nanometers to a few microns. In addition, the average fiber diameter decreases gradually with increasing speed of the collector. Subsequent discussion about the effects of ambient temperature and humidity on the duration of stable jet indicates that moderate values are preferred for generating longer ultrafine PMIA fibers. Compared with the commercial fibers, however, the prepared electrospun PMIA fibers, especially the water-treated ones, show a considerable decrease in thermal and crystalline performance. Further modifications are expected to improve its crystallization and comprehensive properties in future applications.

ACKNOWLEDGMENTS

This work was supported by the National Natural Science Foundation of China (Grant NO. 51076073).

REFERENCES

1. Hodes, G. *Adv. Mater.* **2007**, *19*, 639.
2. Burda, C.; Chen, X. B.; Narayanan, R.; El-Sayed, M. A. *Chem. Rev.* **2005**, *105*, 1025.
3. Whitesides, G. M. *Small* **2005**, *1*, 172.
4. Greiner, A.; Wendorff, J. H. *Angew. Chem. Int. Edit.* **2007**, *46*, 5670.

5. Huang, Z. M.; Zhang, Y. Z.; Kotaki, M.; Ramakrishna, S. *Compos. Sci. Technol.* **2003**, *63*, 2223.
6. Bhardwaj, N.; Kundu, S. C. *Biotechnol. Adv.* **2010**, *28*, 325.
7. Subbiah, T.; Bhat, G. S.; Tock, R. W.; Pararneswaran, S.; Ramkumar, S. S. *J. Appl. Polym. Sci.* **2005**, *96*, 557.
8. Reneker, D. H.; Yarin, A. L.; Fong, H.; Koombhongse, S. *J. Appl. Phys.* **2000**, *87*, 4531.
9. He, J.; Zhou, Y.; Qi, K.; Wang, L.; Li, P.; Cui, S. *Fiber. Polym.* **2013**, *14*, 1857.
10. Ali, U.; Zhou, Y. Q.; Wang, X. G.; Lin, T. *J. Text. I.* **2012**, *103*, 80.
11. Shuakat, M. N.; Lin, T. *J. Nanosci. Nanotechnol.* **2014**, *14*, 1389.
12. Yuan, H.; Zhao, S.; Tu, H.; Li, B.; Li, Q.; Feng, B.; Peng, H.; Zhang, Y. *J. Mater. Chem.* **2012**, *22*, 19634.
13. Carnell, L. S.; Siochi, E. J.; Holloway, N. M.; Stephens, R. M.; Rhim, C.; Niklason, L. E.; Clark, R. L. *Macromolecules* **2008**, *41*, 5345.
14. Sun, Z.; Deitzel, J. M.; Knopf, J.; Chen, X.; Gillespie, J. W. *J. Appl. Polym. Sci.* **2012**, *125*, 2585.
15. Zhou, Q.; Bao, M.; Yuan, H.; Zhao, S.; Dong, W.; Zhang, Y. *Polymer* **2013**, *54*, 6867.
16. Liu, Z.; Li, X.; Yang, Y.; Zhang, K.; Wang, X.; Zhu, M.; Hsiao, B. S. *Polymer* **2013**, *54*, 6045.
17. Yao, L.; Lee, C.; Kim, J. *Fiber. Polym.* **2010**, *11*, 1032.
18. He, B.; Li, J.; Pan, Z. J. *Text. Res. J.* **2012**, *82*, 1390.
19. Chen, K.; Zhang, S. C.; Liu, B. W.; Mao, X.; Sun, G.; Yu, J. Y.; Al-Deyab, S. S.; Ding, B. *RSC Adv.* **2014**, *4*, 45760.
20. Park, Y. S.; Lee, J. W.; Nam, Y. S.; Park, W. H. *J. Appl. Polym. Sci.* **2015**, *132*, DOI: 10.1002/app.41515.
21. Oh, H. J.; Pant, H. R.; Kang, Y. S.; Jeon, K. S.; Pant, B.; Kim, C. S.; Kim, H. Y. *Polym. Int.* **2012**, *61*, 1675.
22. Oh, H. J.; Han, S. H.; Kim, S. S. *J. Polym. Sci. Part B: Polym. Phys.* **2014**, *52*, 807.
23. Sun, D.; Chang, C.; Li, S.; Lin, L. *Nano. Lett.* **2006**, *6*, 839.
24. Zheng, G.; Li, W.; Wang, X.; Wu, D.; Sun, D.; Lin, L. *J. Phys. D Appl. Phys.* **2010**, *43*, 415501.
25. Brown, J. R.; Power, A. *J. Polym. Degrad. Stabil.* **1982**, *4*, 479.
26. Villar-Rodil, S.; Martínez-Alonso, A.; Tascón, J. M. D. *J. Anal. Appl. Pyrol.* **2001**, *58–59*, 105.
27. Villar-Rodil, S.; Paredes, J. I.; Martínez-Alonso, A.; Tascón, J. M. D. *Chem. Mater.* **2001**, *13*, 4297.
28. Schulten, H. R.; Plage, B.; Ohtani, H.; Tsuge, S. *Angew. Makromol. Chem.* **2003**, *155*, 1.
29. Kakida, H.; Chatani, Y.; Tadokoro, H. *J. Polym. Sci. Pol. Phys.* **1976**, *14*, 427.
30. Liu, W. X.; Graham, M.; Evans, E. A.; Reneker, D. H. *J. Mater. Res.* **2002**, *17*, 3206.